Quantification of the *in vivo* kinematics of the superficial femoral artery due to hip and knee flexion using magnetic resonance imaging

G. Choi[1], N. M. Wilson[2], C. P. Cheng[3], R. J. Herfkens[4], and C. A. Taylor[1,2]

[1]Department of Mechanical Engineering, Stanford University, Stanford, CA, United States, [2]Department of Bioengineering, Stanford University, Stanford, CA, United States, [3]Department of Surgery, Stanford University, Stanford, CA, United States, [4]Department of Radiology, Stanford University, Stanford, CA, United States

Introduction

The superficial femoral artery (SFA) is pre-disposed to atherosclerotic disease and hence a frequent site of endovascular stenting procedures. However, due to the interaction between the musculoskeletal system and the vasculature in the lower extremities, this is a challenging location for stents with a recent study reporting that SFA stents fracture at a rate of 37.2% *in vivo* [1]. While local shortening, lengthening and buckling of the SFA have been observed in previous studies [2,3], the kinematic reasons for these complex deformation modes are poorly understood. In this study, we utilized vascular and skeletal magnetic resonance imaging and image processing methods to quantify *in vivo* kinematics of the SFA with respect to the femur.

Methods

Seven male healthy volunteers (56±5 years) were imaged using contrast-enhanced MRA in the supine and bent-leg positions (left decubitus, hip flexion angle: 39±6°, knee flexion angle: 86±6°) using a GE Signa Excite 1.5T scanner. Imaging studies were conducted under a protocol approved by the institutional review board, and informed consent was obtained from all subjects. Twenty mL of gadolinium was injected into the antecubital vein at 3ml/sec followed by a 20 mL flush of saline for each of the two body positions. A time-resolved 3D gradient-recalled MRA sequence (TRICKS) was performed in approximately 4 minutes with the following parameters: 8 ms TR, 1.6 ms TE, 45° flip angle, 512 by 224 acquisition matrix per slice, 2.6 mm slice thickness with 1.3 mm overlap, 8 time-resolved frames, and approximately 19 sec temporal resolution. The TRICKS sequence provides separate image volumes of the femur prior to contrast injection as well as enhanced image contrast of the SFA and branch vessels with contrast.

After correcting for 3D nonlinearities in the gradient field, the femur and SFA image volumes in two different body positions were analyzed to construct their centerline paths using the open-source package SimVascular (www.simvascular.org). A 2D level set segmentation technique was used to find the boundaries of the object and then compute the centroid of the cross section. Fourier smoothing was performed on the centerline connecting the centroids to eliminate spurious irregularities of the centerline. Several distinct branch vessels including the profunda femoris and descending geniculates were identified as fiducial landmarks to determine the axial strain in each segment. Axial strain was defined by the change in the arc length of a segment between branches divided by its original length.

Since the coordinate systems of the supine and bent-leg images differed between the scans, the two image volumes were coregistered based on the femur geometry. The mid-point of the femur centerline was selected as the origin of the local femur coordinate system. A unit vector in the superior-inferior (SI) direction was defined from the most inferior to most superior femur centroid and a unit normal vector of a plane determined by the top, mid and bottom femur centroids was used as a left-right (LR) unit vector. The anterior-posterior (AP) unit vector of the local femur coordinate system was calculated using the cross product of the SI and LR unit vectors.

To achieve the volume coregistration, first, the boundaries of bone marrow fat, which provides bright signal in the femur, were segmented in approximately 1mm intervals and then the cross sectional area was calculated as a function of the arc length of the femur centerline. Because of the convexity of the function of cross sectional femur area in terms of the arc length, an optimal shift can be calculated to find corresponding material points in the supine and bent-leg position. Second, three angles of rotation around the *x*-, *y*-, *z*-axis at the topmost corresponding material point were optimally determined based on an error cost function defined by the distance between the bent-leg femur centerline as a reference and the rotated supine femur centerline. The same lengths of both femur centerlines were sampled in 1mm intervals below the identified topmost corresponding point in the first step. The Nelder-Mead method implemented in Matlab (MathWorks, Inc.) was used for optimization. Finally, the SFA centerline coordinates in the supine position were transformed into the bent-leg position using the resultant optimal translation and rotation matrices. The coregistered SFA coordinates in one configuration provides the relative motion of the SFA with respect to the local femur coordinate associated with the hip and knee flexion. For statistical analysis, the branch points were divided into two groups – the proximal and distal points, which were anterior and posterior to the femur in the supine position, respectively.

Results

Significant shortening of the SFA (-7.1±5.6%, $p<0.001$) was observed under hip and knee flexion. In the supine position, the SFA was 3.9±1.1cm anterior to the femur at the level of the profunda femoris and was 2.9±0.9cm posterior to the femur around the knee. From supine to bent-leg position, the proximal branch points were translated to 0.1±0.5cm anteriorly ($p>0.05$), 0.3±0.7cm left ($p<0.05$) and 0.7±0.7cm inferiorly ($p<0.001$) whereas the distal branch points did not exhibit statiscially significant motion. When the most proximal (profunda femoris) and distal points (most distal geniculate) are considered, hip and knee flexion caused the top of the SFA to move 0.6±0.8cm anteriorly ($p<0.05$), 0.7±1.3cm left ($p>0.05$) and 2.2±0.8cm inferiorly ($p<0.05$), whereas the motion of the bottom of the SFA was not statistically different from zero. The top of the SFA moved 2.4±0.7cm closer to the bottom of the SFA ($p<0.05$).

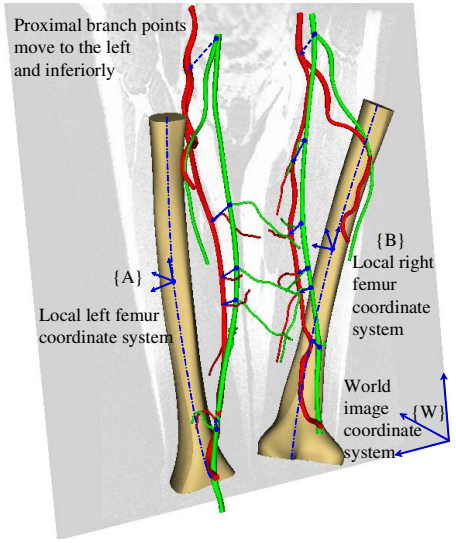

Figure 1. The SFA in supine (green) and bent-leg (red) positions coregistered by the femur.

Discussion

The anatomic location of the SFA and relative kinematic motion with respect to the femur can explain the observed axial shortening in the SFA. Because the SFA trajectory passes anteriorly around the hip joint and continues posteriorly around the knee joint, the hip flexion and knee flexion both contribute to axial shortening of the SFA. We found that the proximal part of the SFA moved more inferiorly than the relatively immobile distal part of the SFA due to hip and knee flexion. Tethering of branches to surrounding skeletal structures around the knee joint can restrict the relative motion compared to the proximal SFA. As a result, the SFA experiences compressive force and hence shortening and buckling occur along the vessel. With regard to the left translation of the proximal SFA, the left decubitus position during the experiment may cause this phenomenon rather than the hip and knee flexion. Due to the weight and compliance of thigh muscles, all soft tissues including vessels were translated left relative to the rigid femur in left decubitus position relative to the supine position. The proposed method to coregister two image volumes has an estimated average error of 0.03±0.01cm after the iterative nonlinear optimization, which is reasonably small compared to the observed translation.

In vivo SFA kinematics obtained in this study provides insight into the interaction between the musculoskeletal and vascular systems. Morever, these methods can be applied to understand muscle deformation, which may influence SFA deformation and subsequently may help elucidate stent fracture mechanisms.

Acknowledgements

This work was supported by the SRI/Stanford Consortium on Stent Failure in the SFA, NIH grant P41 RR09784, the Lucas Center for Magnetic Resonance Imaging at Stanford and GE Medical Systems.

References

[1] Scheinert, D., et al., Journal of American College of Cardiology, 2005. 45(2): p. 312-315
[2] Cheng, C.P., et al., Journal of Vascular Interventional Radiology, 2006. 17: p.979-987
[3] Wensing, P.K.W., et al., Journal of Anatomy, 1995. 186: p. 133-139